Theor Chim Acta (1991) 79: 105–114

Theoretica
Chimica Acta

An *ab initio* study of the molecules P_2O and P_2O^+

Fernando R. Ornellas and Adélia J. A. Aquino
Instituto de Química, Universidade de São Paulo, Caixa Postal 20780, São Paulo, 01498, SP, Brazil

Received May 21, 1990; received in revised form October 15, 1990/Accepted October 16, 1990

Summary. This paper presents a detailed *ab initio* study of the molecules P_2O and P_2O^+ at the Hartree–Fock, and Multi-Reference Single and Double Excitation Configuration Interaction levels. An analysis of the geometries and relative stabilities of both molecules is presented, together with a discussion of the dissociation channels and of the electronic spectrum of linear P_2O. The results for the ionic species P_2O^+ suggest a cyclic geometry for this molecule, as indicated by the calculated vibrational frequencies. The calculations also indicate a surface crossing at a relatively low energy which might lead to P_2O dissociation and may hence be one of the factors contributing to the failure to detect it at room temperatures.

Key words: Phosphorus(I) oxide – Geometry optimization – Dissociation channels – Excitation energies – Electronic spectrum – Vibrational frequencies

1. Introduction

In contrast to the stable and quite well known N_2O molecule [1–3], P_2O is practically an unknown species. Experimentally, the first mention of P_2O was made by Besson [4] at the turn of the last century, but the results of his experiments were questioned by Chapman and Lidbury [5] who were unable to reproduce them. The issue of the existence of P_2O was further debated by Michaelis and Pitsch [6] and by Besson [7]. Based on these old papers, the rare mentions of P_2O in inorganic texts refer to Besson's suboxide as a mixture [8]. Note that P_2O is the putative anhydride of hypophosphorous acid (H_3PO_2), which, along with its salts, is well known.

Using matrix isolation techniques to study the reaction of P_4 with oxygen, Andrews and Whithnall [9] recently recorded the infrared spectra of several oxides, including the suboxides P_2O and P_4O proposed by Besson almost a century ago. A sharp $1197.3\,\mathrm{cm}^{-1}$ band, attributed to an almost pure P=O stretching, was the only fundamental vibration assigned to a linear P_2O structure.

On the theoretical side, preliminary results for P_2O have been reported by Ornellas [10]. Busch and Schoeller [11] have independently carried out a theoretical evaluation of bonding properties of cyclic and linear analogues of N_2O. Although no particular discussion of P_2O was presented in their work, their predicted geometries and relative stabilities obtained at the self-consistent field (SCF) and single-reference single and double excitation configuration interaction levels are nicely concordant with ours. Even more recent work [11] also presents results for the linear and cyclic structures, but mainly addresses the calculation of harmonic frequencies at the SCF and MP2 levels.

In this paper we complement these previous studies with calculations at the SCF and multi-reference single and double excitation configuration interaction (MR-SDCI) levels for both P_2O and its ion P_2O^+. A detailed analysis of the geometries, relative stabilities, binding, dissociation channels and electronic spectrum is presented. The problem of the failure to observe P_2O at room temperature is also addressed.

2. Computation methods

This study has been carried out at both the SCF and MR-SDCI levels. At the SCF level, the geometries were optimized using the gradient of the energy with respect to the nuclear coordinates as implemented in the Hondo/5 program [13]. The optimization was considered complete for changes in the energy gradient smaller than $10^{-4}\,E_h/a_0$. At the MR-SDCI level, the geometries were obtained as the minima in a potential energy surface constructed by varying the phosphorus-phosphorus and phosphorus-oxygen internuclear distances for fixed bond angles. Since these calculations are very time consuming, this search was done only for the linear structure. The MR-SDCI results have been obtained with the Meld codes developed by Davidson and collaborators [14].

Huzinaga's (9*s*, 5*p*) set of cartesian Gaussians [15] contracted to [4*s*, 3*p*] by Dunning [16], plus a set of *d*-type ($\alpha = 0.85$) polarization functions comprised the oxygen basis set. For phosphorus, Huzinaga's (11*s*, 7*p*) set of cartesian Gaussians contracted to [6*s*, 4*p*] by Dunning, plus a set of *d*-type ($\alpha = 0.62$) polarization functions were employed.

Due to symmetry restrictions in the Meld codes, this study was carried out in both the C_{2v} and C_s point group symmetries. The MR-SDCI calculations were made by freezing the canonical molecular orbitals (MOs) corresponding to the 1*s*, 2*s*, 2*p* atomic orbitals on phosphorus and the 1*s* atomic orbital on oxygen. A total of 16 electrons was correlated as single and double excitations from a set of reference configuration state functions considered to be relevant for describing the multiple bond character and the excited states of these molecules. Due to hardware limitations (CYBER 170/730), perturbation theory with energy thresholds of the order of $5 \times 10^{-5}\,E_h$ were used to keep the final wavefunction expansion with 14000 terms. For the same reason, only one set of *d*-type functions was used in the basis sets.

3. Results and discussions

3.1. P_2O, *geometries and energetics*

Total energies for the optimized geometries of P_2O are presented in Table 1. The corresponding structural parameters are given in Table 2. Force constant

Table 1. Total energies (in au) for P_2O. Values in parentheses include the Davidson correction. 756.0 should be subtracted from the listed values

	Linear		Cyclic		Transition state	
	SCF	Correlated	SCF	Correlated	SCF	Correlated
This study	−0.248135	−0.640799 (−0.705375)	−0.238168	−0.632736[e] (−0.696550)	−0.218487	−0.550636[e] (−0.652728)
[11][a]	−0.2390	(−0.6858)	−0.2256	(−0.6742)	−0.2003	(−0.6317)
[12][b]	−0.2318	−0.6739	−0.2233	−0.6573 −0.8112[c] −0.9083[d]		

[a] Basis set: (9*s*, 5*p*)/[5*s*, 3*p*] plus *d*(1.25) for oxygen and (11*s*, 7*p*)/[7*s*, 4*p*] plus *d*(0.5) for phosphorus. Single-reference CI results

[b] Basis set: Pople's 6-31G*. Correlated results at the MP2 level

[c] Basis set: DZ of Huzinaga plus *d*(1.28) for oxygen and *d*(0.465) for phosphorus

[d] Basis set: TZ2P of Huzinaga [15]

[e] SCF optimized geometry was used

Table 2. Optimized geometries for P_2O

	P–P bond length, Å		P–O bond length, Å		PPO bond angle	
	SCF	Correlated	SCF	Correlated	SCF	Correlated
			Linear			
This study	1.846	1.887	1.438	1.468	180	180
[11][a]	1.852		1.446		180	
[12][b]	1.852	1.922	1.446	1.503	180	180
			Cyclic			
This study	1.933		1.709		55.6	
[11][a]	1.938		1.721		55.7	
[12][b]	1.939	2.012 2.007 2.018	1.726	1.776 1.770 1.762	55.9	55.5 55.5 55.1
			Transition state			
This study	2.110		1.472		95.2	
[11][a]	2.118		1.479		95.6	

[a] Correlated results obtained with single-reference CI

[b] Correlated results obtained at the MP2 level

calculations indicate that, of the three converged calculations at the SCF level, the species with highest energy is unstable. Vibrational frequencies corresponding to the true local minima of both linear and cyclic species are listed in Table 3. As discussed in [12], these unscaled harmonic frequencies are expected to be overestimated by about 30%.

Table 3. Unscaled harmonic vibrational frequencies (in cm^{-1}) calculated at the SCF level for P_2O and P_2O^+

P_2O, linear		P_2O, cyclic		P_2O^+, cyclic
201[a]	213[b]	270[a]	303[b]	663[b]
749[a]	752[b]	734[a]	741[b]	977[b]
1429[a]	1451[b,c]	925[a]	938[b]	1098[b]

[a] [12]; [b] This study; [c] The experimental value is 1197.3 cm^{-1}, [9]

The SCF energies found in this study are lower than any of those previously published. In particular, the calculation of Busch and Schoeller [11] also used Huzinaga's basis, but with a different choice of contraction, [5*s*, 4*p*] and a relatively high exponent, 1.25, for the oxygen *d*-function. This choice of exponent makes the *d*-function tighter than the one used in this work (0.85, also recommended by Dunning and Hay [16]) and is certainly the cause of their higher energies and slightly longer bond distances. Although of double-zeta size, that basis set is of the same quality as the split-valence 6-31G* basis set used by Jarret-Sprague et al. [12].

Table 1 includes SDCI [11] and MR-SDCI energies, and perturbation results at the MP2 level [12]. In this study, only the linear structure was optimized at the CI level. The correlated energies for the other structures were calculated at SCF optimized geometries. The MP2 results correspond to optimized geometries. With the exception of the extended basis entries, our results are systematically lower than those published previously. A more useful visualization of the results of Table 1 in the form of relative energies is presented in Fig. 1. The inclusion of correlation effects reduces the energy difference between the cyclic and linear species by only about 10% compared with the SCF value. For the transition state structure (C_s symmetry), hardware limitations forced us to raise the energy threshold to $2.0 \times 10^{-5}\, E_h$ for configuration selection. This threshold, which is about an order of magnitude higher than that used for the linear and cyclic

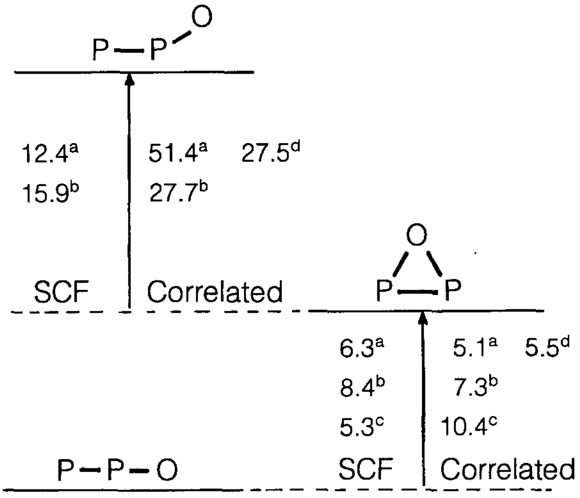

Fig. 1. Relative energies (in kcal/mol) for the optimized structures of P_2O. **a.** This work; **b.** [11]; **c.** [12]; **d.** This work with Davidson correction

structures, is responsible for the relatively high value of the uncorrected CI result, reflecting the absence of a significant number of double and quadruple excitations in the wavefunction.

The MP2 results [12] appear to overestimate the energy of the linear form and/or underestimate the energy of the cyclic structure, the value of 10.4 kcal/mol being about twice that obtained in this study, 5.5 kcal/mol, using MR-SDCI plus the Davidson correction. Since the SCF results are quite close, we are inclined to believe that these structures are not being properly described at the MP2 level. Correlation effects lengthen the SCF bond distances by about 2% at the CI level and by about 4% at the MP2 level. Bond angles are practically unaffected.

In the absence of experimental bond distances and angles for P_2O, it is worth comparing the calculated results with those of known phosphorus and oxygen compounds. The experimental bond distances of P_2 and PO are, respectively, 1.894 Å [17] and 1.476 Å [18]. Our correlated results, 1.887 Å and 1.468 Å for the PP and PO bond distances respectively, are quite close to the bond distances which are characteristic of the triple bond in P_2 and of the double bond in PO. The corresponding MP2 results (1.922 Å and 1.503 Å [12]) are certainly overestimated.

As to the bonding in the linear molecule, there is clear evidence of the participation of all valence orbitals of the phosphorus atoms (see Table 4). The first six molecular orbitals, in order of increasing stability, are: $(4b_1, 4b_2)$ $11a_1$, $(3b_1, 3b_2)$ and $10a_1$ (4π, 11σ, 3π and 10σ in the $C_{\infty v}$ notation). The atomic coefficients of these MOs, listed in Table 5, show that the contribution of the d-type function of the central phosphorus atom to the π-type bonding orbitals between the two phosphorus atoms is significant for the degenerate pair $(4b_1, 4b_2)$. On the other hand, the small magnitude of the coefficients of the functions centered on the peripheral phosphorus atom give the degenerate pair $(3b_1, 3b_2)$ a π-type bonding character involving the central phosphorus and the oxygen atom. As to the $a_1(\sigma)$ orbitals, they seem to be delocalized between the three atoms. This picture is consistent with the valence bond structure $P\overset{--}{=}P{=}O$. Table 4 also suggests the structure $P{\equiv}P^+{-}O^-$.

For the cyclic structure, the P–P bond distance of 1.933 Å at the SCF level is closer to that of the triple bond in P_2 (1.894 Å) than that of the single bond in P_4 (2.21 Å [19]), but is consistent with a "cyclic double bond". Here also the molecular orbitals reveal significant contributions from d-type atomic orbitals, as

Table 4. Mulliken gross atomic populations for P_2O and P_2O^+

	P_2O, cyclic[a]		P_2O, linear[b]			P_2O^+, cyclic[a]	
	P	O	P	P	O	P	O
s	5.640	3.889	5.818	5.086	3.845	5.658	3.852
p_x	3.054	1.469	3.203	2.953	1.708	2.641	1.645
p_y	2.999	1.935	3.203	2.953	1.708	2.988	1.487
p_z	2.583	1.426	2.642	2.751	1.405	2.545	1.512
d	0.342	0.027	0.148	0.528	0.050	0.386	0.069

[a] The molecule is on the yz-plane

[b] The z-axis contains the internuclear distance

Table 5. Atomic coefficients for some molecular orbitals of the linear structure of P_2O

	$10a^1$ ($-$0.679 au)			$11a_1$ ($-$0.518 au)		
	P1	P2	O	P1	P2	O
s	0.014	−0.014	−0.053	−0.017	0.009	−0.009
s	0.043	−0.044	−0.074	−0.053	0.027	−0.014
s	−0.093	0.095	0.220	0.115	−0.060	0.037
s	−0.175	0.184	0.286	0.224	−0.114	0.077
s	0.305	−0.357		−0.391	0.199	
s	0.310	0.154		−0.505	0.294	
p_z	0.016	0.094	0.243	−0.135	0.125	0.150
p_z	0.002	0.012	0.304	−0.021	0.019	0.189
p_z	−0.033	−0.195	0.201	0.285	−0.287	0.145
p_z	0.000	0.038		0.167	−0.121	
d_{zz}	−0.007	−0.014	−0.032	0.060	−0.026	−0.018
d_{yy}	−0.007	0.021	0.007	0.004	0.001	0.002
d_{zz}	−0.007	0.021	0.007	0.004	0.011	0.002
	$3b_1$ ($3b_2$) ($-$0.574 au)			$4b_1$ ($4b_2$) ($-$0.378 au)		
	P1	P2	O	P1	P2	O
$p_{x(y)}$	−0.032	−0.119	0.289	0.167	0.100	0.139
$p_{x(y)}$	−0.006	−0.019	0.385	0.025	0.016	0.168
$p_{x(y)}$	0.072	0.254	−0.295	−0.358	−0.222	0.233
$p_{x(y)}$	0.041	0.183		−0.424	−0.274	
$d_{x(y,z)}$	0.018	0.059	−0.043	−0.065	0.115	−0.014

shown by the Mulliken gross atomic populations listed in Table 4. The calculated PO bond distance, 1.709 Å, is comparable with the observed PO single bond in P_4O_6, 1.65 Å [8].

3.2. P_2O^+, *geometries and energetics*

To our knowledge, these are the first calculations reported for this ionized species; the methodology and basis sets are the same as those used for the neutral molecule. Geometry optimization at the SCF level leads to two stationary points corresponding to a linear and a cyclic structure. Subsequent force constant calculations rule out the linear structure as a minimum. Vibrational harmonic frequencies are listed in Table 3. The geometrical parameters and energies are shown in Fig. 2 together with the Mulliken gross atomic charges for both the ionic and neutral molecules. Atomic populations are shown in Table 4.

Despite the fact that the ionized electron is removed from a bonding π(P–P) molecular orbital, the new P–P bond length (2.009 Å) is not very different from that in the neutral species (1.933 Å). This might imply that the sigma skeleton is the structure determining factor in the molecule. The increase in the $\widehat{POP}$ bond angle of approximately 6° results in an increased overlap between the orbitals describing the P–O bonds, with a concomitant shortening of the bond length to

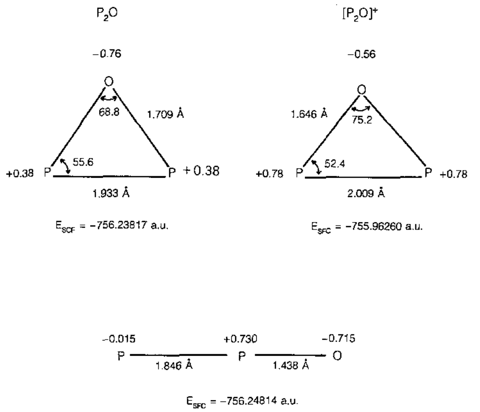

Fig. 2. Geometrical parameters, SCF energies and Mulliken gross atomic charges for P_2O and P_2O^+. $E_{CI}(P_2O^+) = -756.31570$ au

1.646 Å from 1.709 Å in the neutral molecule. The gross atomic charges also clearly increase on the phosphorus atoms in going from the neutral to the ionic molecule. Despite the loss of one electron, this increase is not exactly half an electron for each phosphorus atom because of partial electron migration from the oxygen atom.

As far as we know, there is no experimental evidence for the ionized molecule; nonetheless, the SCF energy difference between the linear structure of neutral species and the cyclic structure of the cation allows us to estimate the adiabatic ionization potential of P_2O to be about 7.5 eV. In this context, the linear structure is less than 0.3 eV more stable than the cyclic one for the neutral molecule.

3.3. Dissociation channels

In this section we examine the possible outcomes of the dissociation of P_2O in its linear geometry. Binding energies were calculated at the SCF and MR-SDCI levels using the counterpoise procedure to correct for basis set superposition errors [20, 21]. Table 6 collects the energies of the fragments allowed by the Wigner–Witmer rule and Fig. 3 shows schematically the various states of P_2O and their dissociation products. Note that the molecular ground state correlates with excited atomic states.

At the SCF level, binding energies of 36.8 and 67.6 kcal/mol (1.60 and 2.93 eV) relative to the excited atomic states were predicted for the P–P and P–O bonds, respectively, in P_2O. Inclusion of the zero-point energy decreases these values to 33.3 and 64.6 kcal/mol (1.44 and 2.80 eV). The use of correlated wavefunctions decreases the energy of the dissociation products of the two different channels by about the same value, 230 kcal/mol (9.97 eV), so that the increase in the binding energy at the CI level relative to the SCF result, 17 kcal/mol (0.74 eV), comes from an increase in the correlation energy of P_2O relative to that of the products. An assessment of the accuracy of our calculations can be made by comparison of our results for the binding energies (D_e) of the molecules P_2 and PO with the experimentally known values of D_0, 116 and 143 kcal/mol (5.03 and 6.20 eV), respectively [17]. As shown in Table 6, our calculations underestimate the dissociation energies of P_2 and PO by about 40 kcal/mol (1.73 eV). Extension of the atomic basis sets to at least a triple zeta

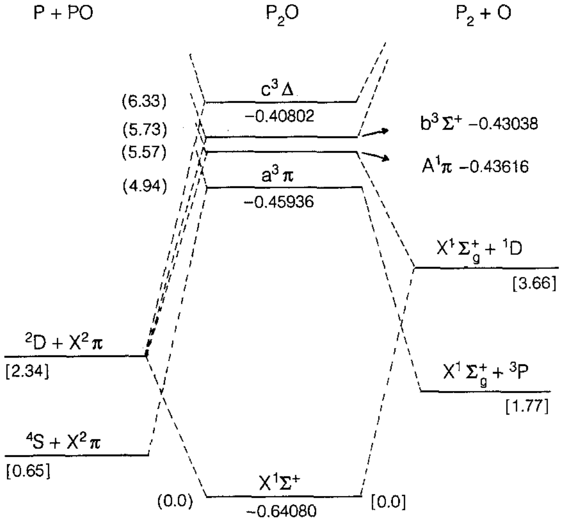

Fig. 3. Energy correlation diagram and vertical excitation energies (in parentheses) for P_2O. Energies for the system PPO are given relative to −756.0 au. Values in parentheses and in brackets are given in eV

level plus another *d*-type function and eventually an *f*-type function plus an enlarged set of configuration state functions would allow a better description of the valence correlation and certainly reduce the above discrepancy. An error of this magnitude has also been found by Lohr [22] for the dissociation energy of PO; using a 6-31G* basis set augmented by diffuse *s*- and *p*-type basis functions for both P and O atoms, values for D_e of 108 and 99 kcal/mol (4.68 and 4.29 eV) were obtained at the MP3 and CISD levels, respectively.

Figure 3 clearly shows that the energy difference between the two lowest $P_2 + O$ dissociation channels is essentially that for the energy separation between the ^1D and ^3P states of oxygen. Table 6 gives 15240 cm^{-1} (1.89 eV) for this energy difference, in quite good agreement with the experimental value of 15868 cm^{-1} (1.97 eV) [23]. Similarly, for the other two dissociation channels (P + PO), the energy difference is that for the separation between the ^4S and ^2D states of phosphorus, 13671 cm^{-1} (1.69 eV; exp.: 11377 cm^{-1} = 1.41 eV, [23]).

Table 6. Energies (in au) of various fragments of the dissociation of P_2O

	SCF	CI
$P(^2D)$	−340.618382	−340.702552
$P(^4S)$	−340.689187	−340.764945
$PO(^2\Pi)$	−415.571191	−415.852109
$P_2(^1\Sigma_g^+)$	−681.421143	−681.653007
$O(^1D)$	−74.719285	−74.853417
$O(^3P)$	−74.801240	−74.922855
$P(^2D)$ + PO	−756.189573	−756.554661
$P(^4S)$ + PO	−756.260378	−756.616954
$P_2O(X^1\Sigma^+)$	−756.248135	−756.640799
ΔE(P–P)^a	36.75	54.08
ΔE(P–O)^a	67.59	84.32

^{a} in kcal/mol

Thus, the error in the relative energies for the two dissociation channels of $P_2 + O$ is expected to be less than 2 kcal/mol, whereas that for the P + PO channels is about 6 kcal/mol. If the energy of the $P(^4S) + PO(^2\Pi)$ channel is corrected by this amount, its separation from the $^1\Sigma^+$ state of P_2O would fall below 10 kcal/mol. Since the errors in the dissociation energies of P_2 and PO are about the same, 40 kcal/mol, it is expected that the relative ordering of these four channels will not change very much with improvements in the wavefunction.

In Fig. 3, the dissociation channel $P(^4S) + PO(X^2\Pi)$ is seen to be about 7.5 kcal/mol lower in energy at the SCF level and about 15 kcal/mol higher in energy at the CI level than the linear P_2O molecule at the equilibrium geometry. Inclusion of the zero-point energy (3.4 kcal/mol) makes the separation between the ground state and this dissociation limit equal to about 4000 cm^{-1} (11.5 kcal/mol) for the correlated wavefunction calculation. These figures suggest that a surface crossing between the $^3\Pi$ and $X^1\Sigma^+$ states might exist at a not so high an energy. Depending on the exothermicity of the reaction leading to the formation of P_2O, population of excited vibrational levels could reduce the barrier further in the newly formed molecule, leading to dissociation via that channel.

In contrast with this situation, N_2O dissociates into N_2 and O [2]. Here, the dissociation limit $N(^2D) + NO(X^2\Pi)$, which correlates with N_2O in its ground state, is about 169 kcal/mol (7.31 eV) higher in energy. The next lowest dissociation limit, $N(^4S) + NO(X^2\Pi)$, is also about 114 kcal/mol (4.93 eV) higher in energy than the ground state. For dissociation into $N_2 + O$, the lowest channel, $N_2(X^1\Sigma^+) + O(^3P)$, is about 39 kcal/mol (1.68 eV) higher in energy and the second lowest, which correlates with the ground state, is about 84 kcal/mol (3.64 eV) higher in energy than the ground state [2]. For N_2O, an MCSCF/CI-$4s3p1d$ treatment of the $X^1\Sigma^+$ state results in 72.0 kcal/mol (3.12 eV) for the NN–O binding energy, which, compared with the experimental value of 86.7 kcal/mol (3.76 eV), represents a recovery of 83% of the binding energy [2]. In the case of P_2O, any further improvements in the wavefunction are unlikely to change the binding energy by more than a fraction of the value observed in going from the SCF to the correlated results. An estimate of 40% of that value, or 6.8 kcal/mol, would increase the P–PO and the PP–O binding energies to about 61 and 91 kcal/mol (2.65 and 3.95 eV), respectively. Comparison of these figures with those for P_2O provides a rationale for the stability of the N_2O molecule and the failure to observe P_2O at room temperature.

Due to the restricted CPU memory in the Cyber 170 computer, the $^3\Pi$ potential energy surface could not be generated with the same accuracy as the ground state surface, preventing precise location of the region of which the two potential surfaces cross.

3.4. *Excited electronic states*

The first few excited electronic states arise from the promotion of electrons at the 4π molecular orbital (MO) to the 12σ and 5π MOs. These configurations and the associated states are

$$\ldots 3\pi^2 11\sigma^2 4\pi^4 \qquad X^1\Sigma^+$$

$$\ldots 3\pi^4 11\sigma^2 4\pi^3 12\sigma^1 \qquad {}^{1,3}\Pi$$

$$\ldots 3\pi^4 11\sigma^2 4\pi^3 5\pi^1 \qquad {}^{1,3}\Sigma^-,\ {}^{1,3}\Delta,\ {}^{1,3}\Sigma^+$$

The relative order of these states and the vertical excitation energies, shown in Fig. 3, were obtained at the MR-SDCI level after a preliminary SCF calculation using the ground state equilibrium geometry. For a given symmetry, the estimated energies of the excited states were obtained as the first few eigenvalues of the hamiltonian matrix. Again, the small main memory of the Cyber 170 computer imposed severe limitations on the final wavefunctions. A relative high energy threshold ($6.5 \times 10^{-5}\ E_h$) had to be used in the configuration selection by perturbation theory, limiting the size of the wavefunction to less than 14000 terms. Therefore, although we believe the ordering to be correct, the relative spacings might be subject to small changes.

With respect to this spectrum, two comparisons with N_2O are worth making. In contrast with P_2O (first excited state $^3\Pi$), the first excited state of N_2O is a $^3\Sigma^+$ state about 6.5 eV higher than the ground state, which correlates with a dissociative state ($N_2(D^2) + NO(X^2\Pi)$) about 0.8 eV higher in energy. Second, the first vertical transition of P_2O fully allowed by the dipole selection rule is predicted to require 5.57 eV, compared with about 8.4 eV for N_2O [2].

Acknowledgements. FRO is grateful to CNPq for a research fellowship and AJAA is thankful to CAPES for a graduate fellowship. The services of the University Computing Center (CCE) are also acknowledged.

References

1. Selwyn GS, Johnston HS (1981) J Chem Phys 74:3791
2. Hopper DG (1984) J Chem Phys 80:4290
3. Peyerimhoff SD, Bunker RJ (1968) J Chem Phys 45:2473
4. Besson MA (1897) CR Acad Sci [Paris] 124, 763; ibid, (1897) 125:1032
5. Chapman DL, Lidbury FA (1899) J Chem Soc 75:973
6. Michaelis A, Pitsch M (1899) Ber 32:337
7. Besson MA (1900) Bull Soc Chim [Paris] 25:582
8. Moeller T (1965) Inorganic Chemistry: An Advanced Textbook. John Wiley, New York
9. Andrews L, Withnall R (1988) J Am Chem Soc 110:5605
10. Ornellas FR. Partial results presented in the poster session of the European Summerschool in Quantum Chemistry, Tjörnarps, Sweden, August 20–September 1, 1989
11. Busch T, Schoeller WW (1989) Z Phys D 13:289
12. Jarret-Sprague SA, Hillier IH, Gould IR (1990) Chem Phys 140:27
13. Dupuis M, Rys J, King HF (1980) QCPE 11:405
14. The MELD code was developed by ER Davidson, SR Langhoff, ST Elbert and LE Murchie with subsequent extensive modifications by D Feller and DC Rawlings
15. Dunning TH (1971) J Chem Phys 55:716
16. Dunning TH, Hay PJ (1977) In: Schaefer HF (ed) Methods of Electronic Structure Theory. Plenum Press, New York
17. Herzberg G (1950) Molecular Spectra and Molecular Structure. I. Spectra of Diatomic Molecules. Van Nostrand Reinhold Co., New York
18. Butler JE, Kawaguchi K, Hirota E (1983) J Mol Spect 101:161
19. Stoll DR, Prophet H (1971) JANAF Thermochemical Tables, NSRDS-NBS 37
20. Boys SF, Bernardi F (1970) Mol Phys 19:553
21. Čársky P, Urban M (1980) Ab Initio Calculations. Springer, Berlin Heidelberg New York, pp 176–7
22. Lohr LL (1984) J Phys Chem 88:5569
23. Moore C (1971) Atomic Energy Levels NSRDS-NBS 35, vol 1 (Washington, DC: US Govt Printing Office)